

Measurements and Modeling of Hyperpolarized 1-13C in the Perfused Lung in Relation to Organ Redox State

Stephen J. Kadlecak¹, Hoora Shaghghi¹, Mehrdad Pourfathi¹, Sarmad Siddiqui¹, Jennia Rajaei¹, Profka Harrilla¹, and Rahim R. Rizi¹
¹Radiology, University of Pennsylvania, Philadelphia, Pennsylvania, United States

INTRODUCTION: Although altered redox state is characteristic of many disease states in many systems, measuring redox in the lung is of particular interest because of that organ's direct exposure to oxidizing agents, its need to produce endogenous reactive oxidizing species for defense against xenobiotics, and the link between lung redox disruption and disease pathogenesis. Hyperpolarized pyruvate is an appealing cytosolic redox measurement tool, because it is directly and rapidly linked to one of the primary redox pairs (NADH:NAD⁺) through lactate dehydrogenase. However, interpretation of the 'apparent' lactate or pyruvate production rate in terms of the hyperpolarized signal is not straightforward. In practice, a wide variety of lung conditions (e.g., ischemia/anoxia, inflammation, hyperoxia, cancer, high blood lactate levels) result in increased hyperpolarized lactate signal, but do not necessarily reflect an altered redox state of the lung tissue.

We seek to clarify the relationship between metabolite signal intensity and the redox state by developing the simplest possible model of hyperpolarized signal dynamics that is consistent with measurements in the isolated, perfused rat lung. Specifically, we address: the relationship between metabolite signal and concentration, between concentrations and redox state, alterations to redox state due to the hyperpolarized agent, and the conditions under which equilibrium approximations are appropriate during the bolus injection. Particular attention is paid to the distinction between flux and 'pool labeling' in the evolution of hyperpolarized signal.

MATERIALS AND METHODS: A total of 25 Sprague-Dawley rats (250-350g) were used for this study. Lungs were excised and placed in a 20-mm NMR tube while perfused with an oxygenated, modified Krebs-Henseleit buffer containing 3% (w/v) fatty acid free BSA (T=36.5 ± 1C, pH=7.4 ± 0.1) and variable amounts of lactate and pyruvate (0-40mM and 0-20mM, respectively) to modify the intracellular concentrations and redox state. Tissue health was monitored using ³¹P spectroscopy. DNP-polarized 1-¹³C pyruvate was diluted in additional buffer (without BSA) yielding a neutral, isotonic solution with a [1-¹³C] pyruvate concentration of 2-32mM which was injected in lieu of the steady-state buffer at 10mL/min. Low flip-angle carbon spectra were acquired for the duration of the hyperpolarized signal and the spectra were fit and analyzed using custom MATLAB routines.

The acquired peak integrals were fit to a kinetic model that accounted for the following processes: flow into and out of the extracellular space, pyruvate and lactate transport into and out of the cell, pyruvate/lactate interconversion via LDH, and pyruvate's conversion to alanine and bicarbonate (flux through PDH).

RESULTS: Several general trends were evident in the data. Most strikingly, the observed lactate signal increased dramatically with exogenous lactate concentration (as shown in **Figure 1, top**). Dependence on injected and steady-state exogenous pyruvate concentration was much weaker, although total metabolite signal approached saturation at high pyruvate concentrations (**Figure 1, bottom, and Figure 2**).

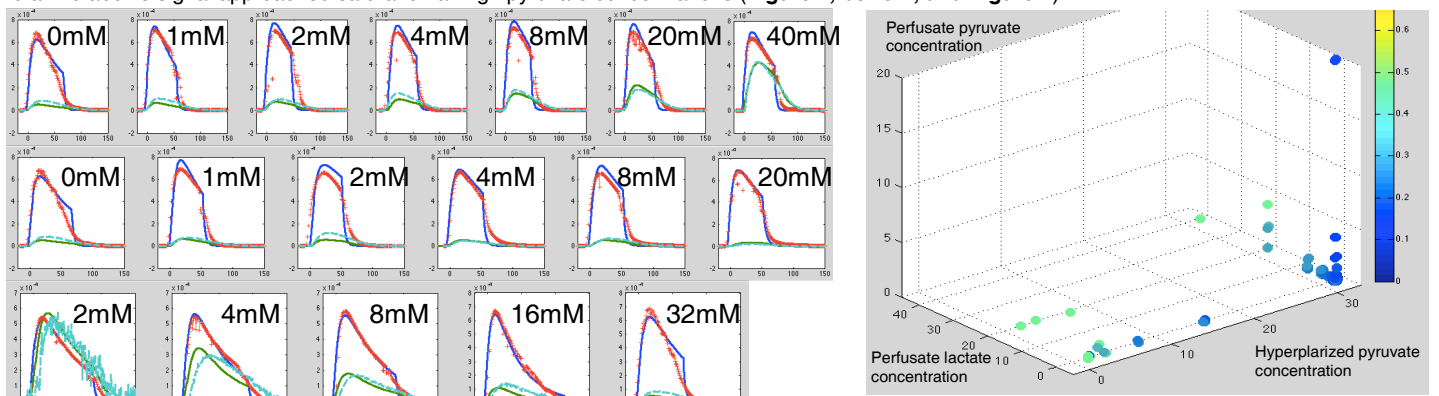


Figure 1 (left): Measured/modeled time-dependence (s) of pyruvate (±30, red/blue) and lactate (dark/sea green) peak as perfusate lactate concentration (top), perfusate pyruvate concentration (middle), and hyperpolarized pyruvate concentration (bottom) is varied as shown in the figure insets.

All of the measurements (red and green traces, above) are well fit by a kinetic model (blue and sea green) which incorporates previously measured characteristics of the rat lung (total NAD and LDH concentrations, glycolysis and uptake rates, and the kinetic parameters describing LDH's interaction with lactate, pyruvate, and cofactors [1]). In the model, the rate of pyruvate/lactate pool exchange takes the form:

$$R = \alpha[Lac] \frac{\beta[Pyr] - G}{\gamma[Pyr] + \delta[Pyr][Lac] + \epsilon[Lac]}$$

where the coefficients $\alpha, \beta, \gamma, \delta, \epsilon$ are depend only on previously measured LDH rate coefficients [1], total NAD and LDH concentrations, and the glycolysis rate G . This form explains the observed near-linear dependence on intracellular lactate concentration ($[Lac]$, or lactate pool size), as well as saturation at high $[Lac]$ and pyruvate levels.

DISCUSSION: We derive expressions which describe the evolution of substrate and metabolite pool polarizations as well as concentrations, and show that in the lung, the observed lactate and pyruvate signal dynamics is entirely explainable in terms of bidirectional pool labeling with negligible contribution from metabolic flux, and minimal dependence on transport characteristics. Furthermore, although intracellular lactate and pyruvate concentrations are at all times representative of cytosolic (NADH:NAD⁺) redox state, polarization equilibrium between the two pools is not readily achieved. Extrapolation based on the modeling results predicts that sensitivity to unperturbed redox state can be achieved through use of low ($\leq \sim 100\mu M$) agent concentration.

REFERENCE: [1] Borgman U, Laidler KJ, Moon TW, Can J Biochem 53 (1975):1196-1206.

Figure 2 (right): A summary of observed Lac/Pyr ratios as concentrations are varied. Color scale is integrated Lac/Pyr signal x 30, all concentrations are mM. General trends toward higher relative lactate labeling are seen in the 'greener' points corresponding to large lactate pool size and low injected (HP) pyruvate.